Mineralogical Magazine, June 2008, Vol. 72(3), pp. 799–808

Gemmological investigation of a synthetic blue beryl: a multi-methodological study

I. ADAMO[1], G. D. GATTA[1,2,*], N. ROTIROTI[1,2], V. DIELLA[2] AND A. PAVESE[1,2]

[1] Dipartimento di Scienze della Terra, Universita' degli Studi di Milano, Italy
[2] CNR-Istituto per la Dinamica dei Processi Ambientali, Milano, Italy

[*Received 27 May 2008; Accepted 14 August 2008*]

ABSTRACT

A multi-methodological investigation of a synthetic Cu/Fe-bearing blue beryl $[^{IV}(Be_{2.86}Cu_{0.14})_{\Sigma=3.00}{}^{VI}(Al_{1.83}Fe^{3+}_{0.14}Mn^{2+}_{0.03}Mg_{0.03})_{\Sigma=2.03}{}^{IV}(Si_{5.97}Al_{0.03})_{\Sigma=6.00}O_{18}\cdot(Li_{0.12}Na_{0.04}\cdot 0.40H_2O)]$ has been performed by means of gemmological standard testing, electron microprobe chemical analyses, laser ablation inductively coupled plasma mass spectroscopy, thermo-gravimetric analyses, infrared spectroscopy and single-crystal X-ray diffraction in order to determine the gemmological properties, crystal structure and crystal-chemistry of this material. The increasing production of marketable hydrothermal synthetic beryls with 'exotic' colours and the small number of studies on the accurate location of chromophores in the crystal structure inspired this multi-methodological investigation. The X-ray structural refinements confirm that the space group of the Cu/Fe-bearing blue beryl is *P6/mcc*, with unit-cell parameters: $9.2483 \leqslant a \leqslant 9.2502$ Å and $9.2184 \leqslant c \leqslant 9.2211$ Å. The analysis of the difference Fourier maps of the electron density suggests that Cu is located at the tetrahedral site (Wyckoff 6*f* position) along with Be, whereas Fe shares the octahedral site with Al (4*c* position). No evidence of extra-framework Cu/Fe-sites (i.e. channel sites) has been found. The Li is probably located at the extra-framework 2*b* site. Infrared spectra show that the H_2O molecules are present with two configurations: one with the H···H vector oriented ||[0001] and the other with H···H vector oriented ⊥[0001].

KEYWORDS: synthetic beryl, crystal chemistry, ICP-MS, IR spectroscopy, single-crystal XRD, structurally incorporated water.

Introduction

BERYL (ideal composition: $Be_3Al_2Si_6O_{18}$; space group: *P6/mcc*) is a common accessory mineral of pegmatitic rocks. The crystal structure of beryl consists of 6-membered rings of Si tetrahedra, perpendicular to the [0001] axis, linked by Al octahedra and Be tetrahedra to form a three-dimensional framework (Fig. 1). Alkali cations, water and carbon dioxide molecules often occupy 'extra-framework' sites, placed within the 6-membered ring channel parallel to [0001]. Several studies have been carried out on the crystal-chemistry and thermo-elastic behaviour of natural and synthetic beryls with a wide variety of extra-framework populations (Bragg and West, 1926; Wood and Nassau, 1967, 1968; Gibbs *et al.*, 1968; Goldmann *et al.*, 1968; Morosin, 1972; De Almeida *et al*., 1973; Hawthorne and Černý, 1977; Aines and Rossman, 1984; Brown and Mills, 1986; Hazen *et al.*, 1986; Aurisicchio *et al.*, 1988; Evdokimova *et al*., 1989; Schmetzer, 1989; Sanders and Doff, 1991; Sheriff *et al.*, 1991; Artioli *et al.*, 1993, 1995; Charoy *et al.*, 1996; Ferraris *et al*., 1999; Kolesov and Geiger, 2000; Prencipe, 2002; Černý *et al.*, 2003; Andersson, 2006; Gatta *et al*., 2006).

Because of the commercial value of beryl, a large number of synthetic samples is permanently present on the market (Koivula *et al.*, 2000). The production of marketable synthetic beryls from

* E-mail: diego.gatta@unimi.it
DOI: 10.1180/minmag.2008.072.3.799

© *2008 The Mineralogical Society*

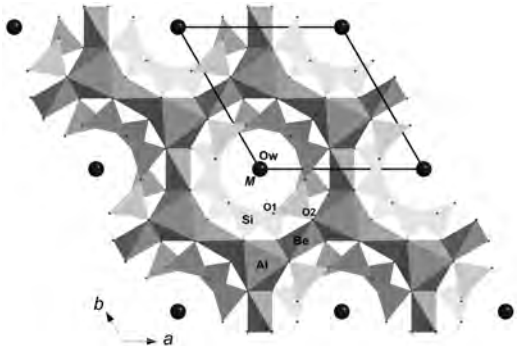

FIG. 1. The crystal structure of beryl viewed down [0001]. The extra-framework Ow and *M* sites are overlapped in this view.

hydrothermal growth techniques dates back to the end of 1980s, and the different stones' colourations are obtained using chromophoric dopants such as, for instance, V, Cr, Mn, Fe, Co, Ni and Cu (Koivula and Kammerling, 1988; Nassau, 1990).

Notwithstanding the relevant role that synthetic beryls play as a gem material and the increasing interest in 'exotic' colourations, comparatively few studies have been found in the literature which investigate the accurate location of the chromophores in the crystal structure, even though this information is crucial to model and understand the mechanisms governing the beryl's colouration. The aim of the present study is to present a multi-methodological investigation of a synthetic Cu/Fe-bearing blue beryl, by means of gemmological standard testing, electron microprobe analysis (EMPA), laser ablation inductively coupled plasma mass spectroscopy (LA-ICP-MS), thermo-gravimetric analysis (TGA), infrared (IR) spectroscopy and single-crystal X-ray diffraction (XRD), in order to provide both mineralogical and gemmological characterizations of this synthetic stone.

Experimental methods

Synthetic dark blue beryl crystals (sample M2), from the same production cycle and kindly provided by A. Malossi (Malossi Gemme Create, Milan), were used for the present study (Fig. 2). This material was grown hydrothermally at ~580ºC in a small rotating autoclave lined with gold and copper and carefully sealed. A natural Brazilian Li-bearing beryl was added as feed to the alkaline growth solution along with Cu, Fe and Mn salts. Typically, large beryl crystals (average size ~70 mm × 60 mm × 15 mm) were grown in ~40 days.

The sample was examined by standard gemmological methods to determine the optical properties (refractive indices, birefringence and pleochroism), specific gravity and ultraviolet

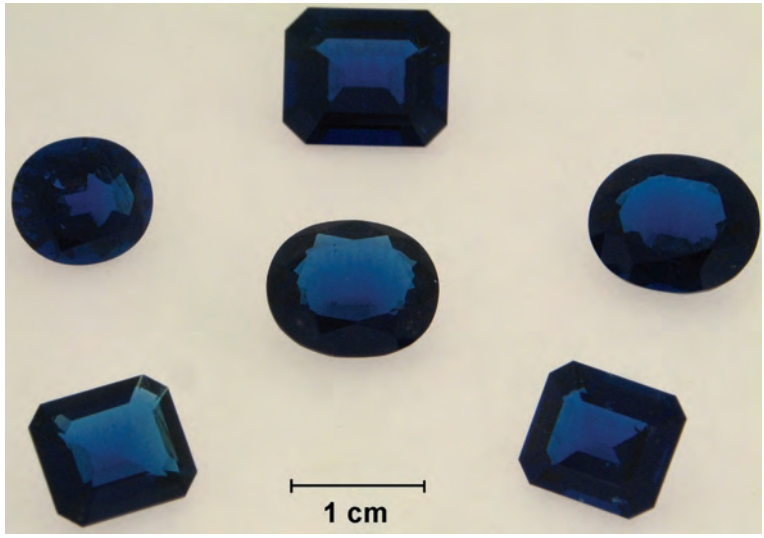

FIG. 2. Some synthetic blue beryls (2.70–4.35 ct) from the same production cycle. The oval-shaped beryl on the left side is the sample M2 used for the present investigation.

fluorescence. The refractive indices were measured with a Kruss refractometer using sodium light (589 nm) from a Leitz lamp, and methilene iodide as a contact liquid (R.I. = 1.79). A Mettler hydrostatic balance was used to determine the density of the stone, whereas pleochroism measurements were carried out by a calcite dichroscope. The ultraviolet fluorescence was investigated with a short (254 nm) and long (366 nm) wavelength ultraviolet Wood lamp.

The quantitative chemical analysis in wavelength dispersive spectroscopy (WDS) mode was performed using a JEOL JXA-8200 electron microprobe (EMPA-WDS) at the Earth Science Department of the University of Milan, Italy (ESD-MI). The system was operated with an accelerating voltage of 15 kV, a beam current of 15 nA and a counting time of 20 s on the peaks and 5 s on the backgrounds. A series of minerals was used as standards: K-feldspar for K, olivine for Mg, wollastonite for Si and Ca, omphacite for Na, ilmenite for Ti, fayalite for Fe, pollucite for Cs, anorthite for Al, rhodonite for Mn and pure Rb, V, Cr, Ni, Co and Cu. The results were processed for matrix effects using a conventional ZAF routine in the JEOL program series.

The LA-ICP-MS measurements were performed at the CNR-Geoscience and Georesource Institute, Unit of Pavia, Italy. The probe comprises an Elan DRC-e mass spectrometer coupled with a Q-switched Nd:YAG laser source (Quantel Brilliant), whose fundamental emission (1064 nm) is converted to 266 nm by two harmonic generators. Helium was used as a carrier gas, mixed with Ar downstream of the ablation cell. Calibration was performed using NIST SRM 610 glass as an external calibration sample in combination with an internal standardization based on Si, previously fixed by EMPA-WDS. The detection limits lie within 100–500 ppb for Sc, Ti and Cr; 10–100 ppb for V, Rb, Sr, Zr, Cs, Ba, Gd and Pb; 1–10 ppb for Y, Nb, La, Ce, Nd, Sm, Eu, Tb, Dy, Er, Yb, Hf and Ta; and usually <1 ppb for Pr, Ho, Tm, Lu, Th and U. Precision and accuracy were both better than 10% for concentrations at the ppm scale. The following masses (isotopes) have been analysed: ^{7}Li, ^{9}Be, ^{23}Na, ^{24}Mg, ^{27}Al, ^{29}Si, ^{35}Cl, ^{39}K, ^{44}Ca, ^{45}Sc, ^{49}Ti, ^{51}V, ^{53}Cr, ^{55}Mn, ^{56}Fe, ^{59}Co, ^{60}Ni, ^{63}Cu, ^{85}Rb and ^{133}Cs.

Thermo-gravimetric analyses were performed at the Department of Chemistry of the University of Perugia, Italy, with a NETZSCH STA 449C instrument, using 8.003 mg of powdered sample (crystal size 10–15 μm) previously dried at 130ºC for 4 h. The thermal curve (weight loss *vs. T*, obtained in air and with a *T*-increase rate of 1ºC/min) shows a negative slope trend, which starts flattening at ~1100ºC and stretches up to 1200ºC.

The infrared (IR) spectroscopic investigation in the mid-IR (4000–400 cm^{-1}) range was carried out using a Nicolet Nexus Fourier transform infrared (FTIR) spectrophotometer at the ESD-MI. The spectra were collected in transmission mode by KBr compressed pellets with a sample-to-KBr ratio of 1:100 in weight, and operating at a resolution of 4 cm^{-1}.

Three high-quality crystals were selected for the XRD experiments. Diffraction intensity data were collected with an Oxford Diffraction-Xcalibur diffractometer equipped with a CCD, using a graphite monochromator and Mo-$K\alpha$ radiation, operated at 50 kV and 40 mA. A combination of ω and φ scans was used in order to maximize sampling of reciprocal space, fixing a step size of 0.8º, a time of 6 s/frame and a crystal–detector distance of 80 mm. Bragg reflections were collected in the range $2º < 2\theta < 70º$. A metrically hexagonal lattice was observed for all three crystals (with c/a <1, Table 1) and the systematic extinction conditions were consistent with space group *P*6/*mcc*. The diffraction data were integrated with the computer program *CrysAlis* (Oxford Diffraction, 2005) and then corrected for Lorentz-polarization effects. A further analytical absorption correction was performed by Gaussian integration based upon the physical description of the crystal (*CrysAlis*; Oxford Diffraction, 2005). After corrections, the discrepancy factors between symmetry-related diffraction intensities (Laue class 6/*mmm*) were $R_{int} \approx 0.061$, $R_{int} \approx 0.049$ and $R_{int} \approx 0.064$ for the crystal M2-1, M2-2 and M2-3, respectively (Table 1).

Results

Gemmological properties

The 2.70 ct gem-quality synthetic beryl investigated in the present study is transparent with dark violet-blue colour and vitreous lustre. It is uniaxial negative, with refractive indices ω = 1.590 and ε = 1.582 and birefringence 0.008. The dichroism is strong, with a dark-blue violetish colour along the extraordinary ray and a pale blue along the ordinary ray. The measured density is 2.77 g/cm^3. The gem is non-fluorescent in short/

TABLE 1. Details of the single-crystal XRD data collections and refinements of the beryl crystals M2-1, M2-2 and M2-3.

	M2-1	M2-2	M2-3
Diffractometer	Xcalibur CCD	Xcalibur CCD	Xcalibur CCD
X-ray radiation	Mo-$K\alpha$	Mo-$K\alpha$	Mo-$K\alpha$
T (K)	298	298	298
Scan type	ω/φ	ω/φ	ω/φ
Scan width (º/frame)	0.8	0.8	0.8
Exposure (s/frame)	6	6	6
Temperature (K)	292	292	292
Space group	*P6/mcc*	*P6/mcc*	*P6/mcc*
Z	2	2	2
a (Å)	9.2502(13)	9.2489(8)	9.2483(14)
c (Å)	9.2184(19)	9.2211(7)	9.2193(13)
Maximum 2θ (º)	70	70	70
Extinction correction factor	0.014(4)	0.084(9)	0.033(5)
	$-13 \leqslant h \leqslant 13$	$-11 \leqslant h \leqslant 11$	$-12 \leqslant h \leqslant 12$
	$-14 \leqslant k \leqslant 14$	$-14 \leqslant k \leqslant 14$	$-14 \leqslant k \leqslant 14$
	$-12 \leqslant l \leqslant 12$	$-14 \leqslant l \leqslant 14$	$-13 \leqslant l \leqslant 13$
Measured reflections	15125	15114	15105
Unique reflections	495	522	498
Unique reflections with $F_o>4\sigma(F_o)$	431	474	431
R_{int}	0.061	0.049	0.064
Number of l.s. parameters	34	34	34
$R_1(F)$, with $F_o>4\sigma(F_o)$	0.0411	0.0322	0.0374
$wR_2(F^2)$, all data	0.1005	0.0870	0.0792
GooF	1.179	1.284	1.298
Residuals (e^-/Å^3)	+0.32/−0.36	+0.51/−0.57	+0.31/−0.47

Note: $R_{int} = \Sigma|F^2_{obs} - F^2_{obs}(mean)|/\Sigma[F^2_{obs}]$; $R_1 = \Sigma(|F_{obs}| - |F_{calc}|)/\Sigma|F_{obs}|$;
$wR_2 = [\Sigma[w(F^2_{obs} - F^2_{calc})^2]/\Sigma[w(F^2_{obs})^2]^{0.5}$, $w = 1/ [\sigma^2(F^2_{obs}) + (a*P)^2 + b*P]$,
$P = (\text{Max } (F^2_{obs}, 0) + 2*F^2_{calc})/3$

long wavelength ultraviolet radiation. These gemmological properties are consistent with those of natural aquamarine (Webster, 2006).

Chemical composition

Table 2 shows the chemical composition of the synthetic M2 beryl. The sample is characterized by the presence of large Cu and Fe contents (1.47−3.13 wt.% CuO and 1.82−2.11 wt.% Fe_2O_3). We observed an inverse correlation between CuO and BeO amounts, which suggests an isomorphic substitution at the Be site, in agreement with the chemical consideration of Schmetzer *et al.* (2006). Alkali cations, as Li, Na and Mg are also present (average 0.31, 0.20, 0.19 wt.% for Li_2O, Na_2O and MgO, respectively), as well as manganese (MnO average 0.12 wt.%). Among the measured trace elements, Ni and Cl are the most relevant (~800 and 500 wt. ppm, respectively). Weight-loss measurements indicate a H_2O content of 1.29 wt.%.

IR spectra

Infrared spectroscopy of the synthetic M2 blue beryl over the diagnostic range of fundamental water stretching vibrations (3800−3500 cm^{-1}) provides patterns with two dominant absorption bands at 3698 and 3595 cm^{-1} (Fig. 3), assignable to ν_3 (asymmetric stretching) and ν_1 (symmetric stretching) zone-centre modes, respectively, of water molecules whose H···H vector occurs in two configurations, one parallel ('type I') and the other normal ('type II') to [0001] (Wood and Nassau, 1967, 1968; Farmer, 1974; Aines and Rossman, 1984; Schmetzer, 1989; Schmetzer and Kiefert, 1990; Aurisicchio *et al.*, 1994; Charoy *et al.*, 1996; Mashkovtsev and Smirnov, 2004; Schmetzer *et al.*, 2006). The structured band at

TABLE 2. Average chemical composition of the synthetic M2 blue beryl sample.

	Wt.% oxide	Atoms p.f.u.		Wt. ppm
SiO_2	64.22	5.968	^{35}Cl	511.26
Al_2O_3	16.75	1.835	^{39}K	46.54
Fe_2O_3	1.95	0.136	^{44}Ca	145.87
MnO	0.12	0.026	^{45}Sc	29.13
Na_2O	0.20	0.036	^{49}Ti	70.79
MgO	0.19	0.026	^{51}V	4.25
CuO	1.98	0.139	^{53}Cr	70.57
BeO	12.79	2.856	^{59}Co	12.15
Li_2O	0.31	0.116	^{60}Ni	799.18
H_2O	1.29	0.400	^{85}Rb	7.37
Tot.(1)	99.80		^{133}Cs	117.22
			Tot.(2)	1814.33
Tot.(1)+Tot(2)	99.98			

$^{IV}(Be_{2.86}Cu_{0.14})_{\Sigma=3.00}{}^{VI}(Al_{1.83}Fe^{3+}_{0.14}Mn^{2+}_{0.03}Mg_{0.03})_{\Sigma=2.03}{}^{IV}(Si_{5.97}\ Al_{0.03})_{\Sigma=6.00}O_{18}\cdot(Li_{0.12}Na_{0.04}\cdot 0.40H_2O)$

Note: Values of major and minor elements are those obtained by LA-ICP-MS, except for SiO_2 and Al_2O_3 wt.% (determined by EMPA-WDS) and H_2O (measured by TGA).
Total Fe is calculated as Fe_2O_3; however, charge balance suggests $Fe^{3+}_{0.07}$ + $Fe^{2+}_{0.07}$

3663 cm^{-1}, with a shoulder at 3652 cm^{-1}, is not a single absorption but more likely a combination of at least two absorption bands ascribable to type-II H_2O and/or hydroxyl ions (Schmetzer and Kiefert, 1990; Aurisicchio *et al.*, 1994). However, the interpretation of the nature of this band is not unique (Schmetzer and Kiefert, 1990; Aurisicchio *et al.*, 1994: Andersson, 2006).

The diagnostic band of CO_2 at ~2360 cm^{-1} is absent in our synthetic beryl specimen (Wood and Nassau, 1967, 1968; Aines and Rossman, 1984; Andersson, 2006; Gatta *et al.*, 2006).

Structure refinement

X-ray structure refinements of three M2 blue beryl crystals (i.e. M2-1, M2-2 and M2-3, Table 1) were carried out by means of the *SHELXL-97* package (Sheldrick, 1997), in the space group *P*6/*mcc*, first adopting isotropic displacement parameters and starting from the atomic coordinates of Gatta *et al.* (2006). Neutral X-ray scattering factors of the atoms from the *International Tables for Crystallography C* (Wilson and Prince, 1999) were used. A correction for secondary isotropic extinction was applied according to the Larson's

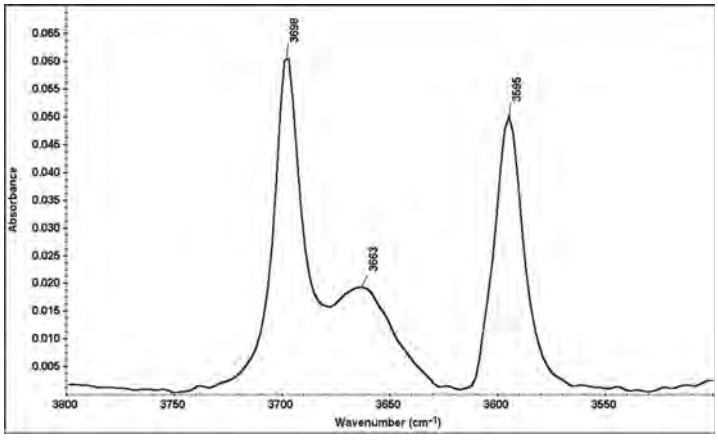

FIG. 3. The mid-IR spectrum (3800−3500 cm^{-1}) in transmission mode of the synthetic M2 blue beryl.

formalism (1970). The initial refinement cycles were performed taking into account the framework atoms only (i.e. fully empty channels), attributing Be and Al to tetrahedral (1/2, 0, 1/4, 6*f* position) and octahedral (2/3, 1/3, 1/4, 4*c* position) sites, respectively. Anisotropic thermal parameters were then introduced for all atoms in the successive refinement stages. The convergence was rapidly achieved and the variance-covariance matrix did not show strong correlations between the refined parameters (scale factor, atomic position of the framework sites and their displacement parameters). The structure-refinement strategy ignoring extra-framework atoms led to four intense residual peaks, revealed by the difference Fourier map of the electron density (Fig. 4); two are located in the [0001] channel (~1.4 e^-/Å^3 at 0, 0, 0, 2*b* position; ~2.8 e^-/Å^3 at 0, 0, 1/4, 2*a* position), one at the tetrahedral site (~2.0 e^-/Å^3) and the latter at the octahedral site (~0.95 e^-/Å^3). All of the three samples studied provided similar results. Further refinements were performed assigning the X-ray scattering factor of oxygen to the 2*a* position and that of lithium to the 2*b* position. In addition, the tetrahedral site population was refined assuming the co-presence of Be and Cu, and that of the octahedral site introducing Fe to Al. Such atomic arrangement led to a rapid achievement of convergence, a decrease of the correlation between the refined parameters (as shown by the variance-covariance matrix) and an enhancement of the agreement factors (R_1, wR_2, GooF). A further inspection of the difference Fourier maps brought to light residual peaks with almost insignificant values (Fig. 5, Table 1), and the bi-elemental tetrahedral and octahedral populations led to a more reliable description of their anisotropic thermal displacement factors. Structure parameters from refinements are set out in Table 3. Relevant bond distances and angles are listed in Tables 4 and 5 (deposited with the Principal Editor and found at http://www.minersoc.org/pages/e_journals/dep_mat_mm.html), respectively. Table 6 (also deposited) provides observed and calculated structure factors.

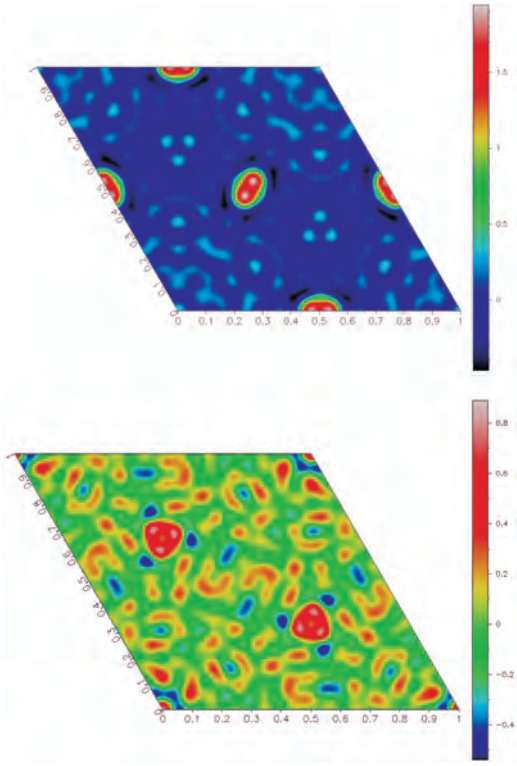

FIG. 4. Difference Fourier maps of the electron density (e^-/Å^3) of beryl (data from the M2-2 crystal) at z = 1/4 after the first cycles of anisotropic refinement, (above) considering a Cu/Fe-free structure and (below) after the assignment of Cu at the Be site (i.e. at x = 1/2, y = 0). For the Cu/Fe-free structure, a residual peak of around +2.0 e^-/Å^3 at x = 1/2, y = 0 is evident. After the assignment of Cu at the Be site, a residual peak of around +0.9 e^-/Å^3 located at the Al site (i.e. x = 2/3, y = 1/3) is still evident. Note that the colour scale is different for the two maps.

Discussion and conclusions

The diffraction intensities and structural refinements show that this synthetic Cu/Fe-bearing blue

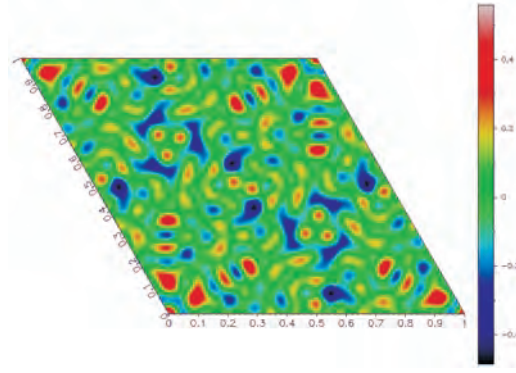

FIG. 5. Difference Fourier maps of the electron density (e^-/Å^3) of beryl (data from the M2-2 crystal) at z = 1/4 at the end of the refinement (i.e. after the assignment of Cu at the Be site and Fe at the Al site).

TABLE 3. Refined positional and displacement parameters (Å^2) of the synthetic blue beryls M2-1, M2-2 and M2-3.

Site (Wyckoff pos.)	x	y	z	Site occupancy	U_{11}	U_{22}	U_{33}	U_{23}	U_{13}	U_{12}	U_{eq}/U_{iso}
Si (12*l*)	0.38706(8)	0.11623(9)	0	1.0	0.0060(3)	0.0061(3)	0.0054(4)	0	0	0.0033(2)	0.0057(2)
	0.38706(7)	0.11627(7)	0	1.0	0.0064(2)	0.0060(2)	0.0067(3)	0	0	0.0033(2)	0.0063(2)
	0.38708(7)	0.11635(7)	0	1.0	0.0063(3)	0.0061(1)	0.0070(1)	0	0	0.0033(2)	0.0064(2)
Be (6*f*)	½	0	¼	Be 0.953(3) Cu 0.047(3)	0.0126(3)	0.005(1)	0.006(2)	0	0	0.0025(7)	0.0088(9)
	½	0	¼	Be 0.952(2) Cu 0.048(2)	0.012(1)	0.006(1)	0.0082(9)	0	0	0.0032(5)	0.0097(7)
	½	0	¼	Be 0.943(2) Cu 0.057(2)	0.014(1)	0.006(1)	0.007(1)	0	0	0.0030(6)	0.0098(7)
Al (4*c*)	2/3	1/3	¼	Al 0.942(6) Fe 0.058(6)	0.0061(4)	0.0061(4)	0.0042(7)	0	0	0.0031(2)	0.0055(4)
	2/3	1/3	¼	Al 0.941(6) Fe 0.059(6)	0.0062(4)	0.0062(4)	0.0053(4)	0	0	0.0031(2)	0.0059(3)
	2/3	1/3	¼	Al 0.946(5) Fe 0.054(5)	0.0064(4)	0.0064(4)	0.0046 (5)	0	0	0.0032(2)	0.0058(3)
O1 (12*l*)	0.30799(25)	0.23577(23)	0	1.0	0.0120(9)	0.0108(9)	0.019(1)	0	0	0.0077(8)	0.0130(5)
	0.30768(20	0.23559(18)	0	1.0	0.0139(7)	0.0119(7)	0.0194(7)	0	0	0.0095(7)	0.0137(3)
	0.30732(21)	0.23550(18)	0	1.0	0.0149(8)	0.0114(8)	0.0193(7)	0	0	0.0093(7)	0.0140(4)
O2 (24*m*)	0.49789(16)	0.14549(16)	0.14496(17)	1.0	0.0128(6)	0.0107(6)	0.0094(8)	−0.0026(5)	−0.0039(5)	0.0071(5)	0.0104(3)
	0.49762(12)	0.14536(13)	0.14492(11)	1.0	0.0135(5)	0.0120(5)	0.0102(4)	−0.0030(3)	−0.0047(3)	0.0079(2)	0.0112(4)
	0.49793(13)	0.14567(13)	0.14483(12)	1.0	0.0141(5)	0.0117(5)	0.0113(5)	−0.0030(4)	−0.004(4)	0.0079(3)	
	0.0117(4)										
Ow (2*a*)	0	0	¼	0.44(4)							0.08(1)
	0	0	¼	0.49(4)							0.09(1)
	0	0	¼	0.48(4)							0.09(1)
M (2*b*)	0	0	0	1.26 e^-							0.07(2)
	0	0	0	1.35 e^-							0.05(1)
	0	0	0	1.38 e^-							0.09(2)

Note: For each site, the values from top to bottom correspond to the refinement based on the diffraction data of the crystal M2-1, M2-2 and M3-3, respectively. The anisotropic displacement factor exponent takes the form: $-2\pi^2[(ha^*)^2U_{11} + \cdots + 2hka^*b^*U_{12}]$. U_{eq} is defined as one-third of the trace of the orthogonalized U_{ij} tensor. The *M* site occupancy is given as refined numbers of electrons, calculated on the basis of the Li-scattering factor.

TABLE 4. Relevant bond distances (Å).

Si–O1	1.5992(19)
	1.5990(14)
	1.5982(15)
Si–O1′	1.6021(19)
	1.6023(14)
	1.6035(15)
Si–O2 (2)	1.6225(15)
	1.6213(10)
	1.6215(11)
Be–O2 (×4)	1.6660(14)
	1.6663(10)
	1.6678(11)
Al–O2 (×6)	1.9187(13)
	1.9203(10)
	1.9181(11)

Note: For each site, the values from top to bottom correspond to the refinement based on the diffraction data of the crystals M2-1, M2-2 and M3-3, respectively.

beryl maintains the space group and general structural arrangement of its natural counterpart. Refractive indices and density of the specimens investigated here are similar to those typical of natural aquamarine samples. Careful inspections of the difference-Fourier maps of the electron density show, unambiguously, that Cu and Fe are located at the tetrahedral (6*f*) and octahedral (4*c*) sites, respectively, as suggested by Evdokimova *et al*. (1989) and Artioli *et al.* (1993). The average populations, over three samples, of Cu and Fe at the Be- and Al sites are ~0.15 and ~0.12 atoms per formula unit (a.p.f.u), respectively, in good agreement with the chemical analysis (~0.14 a.p.f.u. for both, Tables 2 and 3). No evidence of extra-framework Cu-Fe sites (i.e. channel sites) has been observed. Ni reasonably lies at the octahedral site in substitution of Al and Fe.

The presence of Cu at the tetrahedral site and Fe^{3+} at the octahedral site is also supported by the refined bond distances. On the basis of single-crystal neutron diffraction data of an almost pure beryl, Gatta *et al.* (2006) reported Be–O = 1.6545(12) and Al–O = 1.9072(11) Å. The refined bond distances of our Cu/Fe-bearing beryls lie within the ranges $1.6660(14) \leqslant T_{6f}\text{–O} \leqslant 1.6678(11)$ Å and $1.9181(11) \leqslant M_{4c}\text{–O} \leqslant 1.9203(10)$ Å (Table 4). Since the tetrahedral Cu–O bond distance is significantly larger than that of Be–O (i.e. Cu–O >1.98 Å, Ismunandar *et al.*, 1999) and the octahedral $Fe^{3+/2+}$–O bond distance is slightly larger than that of Al–O (i.e. $Fe^{3+/2+}$–O >2.0 Å, Fleet, 1981), we can infer that the refined bond lengths for our blue beryl crystals support the location of Cu at the tetrahedral and Fe at the octahedral sites, respectively.

The channel content distributes over two extra-framework sites: the first is occupied by water molecules (2*a*) and the second (2*b*) mainly by alkali cations (*M* site). Such partitioning agrees with those found in previous studies (Gibbs *et al.*, 1968; Morosin, 1972; Hawthorne and Černý, 1977; Brown and Mills, 1986; Evdokimova *et al*., 1989; Sanders and Doff, 1991; Artioli *et al.*, 1993, 1995; Andersson, 2006; Gatta *et al*., 2006). The amount of water calculated by our structural refinements is comparable with that obtained by the weight-loss measurements and ranges from 0.40 to 0.49 molecules per formula unit (p.f.u.). Moreover, the FTIR spectroscopy provides useful information about the configurations of water molecules in the [0001] channel. We found both type-I and type-II H_2O molecules, as expected for low-alkali-bearing natural and synthetic hydrothermally-grown beryls (Schmetzer and Kiefert, 1990). Our structural refinements assign Li at the extra-framework 2*b*-site. The occurrence of Li in the channel sites has been assumed previously (Manier-Glavinaz *et al.*, 1989; Sheriff *et al*., 1991). However, Sheriff *et al*. (1991), on the basis of ^{7}Li MAS NMR spectroscopy, showed that Li occurs both as a framework constituent (replacing Be) and as a channel species at the 2*b*-position. More recently, Andersson (2006) indicated the 2*b* site as the position of Li in the beryl channel.

The issues discussed here support the importance of resorting to a multi-methodological approach to provide an unequivocal description of a beryl variety, including when its macroscopic features are involved, as is the case for materials relevant to gemmology.

Acknowledgements

The authors thank Mr A. Malossi for providing the synthetic sample investigated here and Dr F. Costantino and Prof. R. Vivani (Department of Chemistry, Perugia) for the thermo-gravimetric analysis. Dr A. Zanetti (CNR, Pavia) is acknowledged for the LA-ICP-MS analysis. Prof. R. Bocchio (ESD, Milan) is thanked for her advice. The Associate Editor (E. Sokolova) and three reviewers (L. Groat, A. Likhacheva and

G. Redhammer) are thanked for their suggestions. The Italian Ministry of University and Research (MIUR) and National Research Council (CNR) are acknowledged for their financial support.

References

Aines, R.D. and Rossman, G.R. (1984) The high-temperature behaviour of water and carbon dioxide in cordierite and beryl. *American Mineralogist*, **69**, 319–327.

Andersson, L.O. (2006) The position of H^+, Li^+ and Na^+ impurities in beryl. *Physics and Chemistry of Minerals*, **33**, 403–416.

Artioli, G., Rinaldi, R., Ståhl, K. and Zanazzi, P.F. (1993) Structure refinements of beryl by single-crystal neutron and X-ray diffraction. *American Mineralogist*, **78**, 762–768.

Artioli, G., Rinaldi, R., Wilson, C.C. and Zanazzi, P.F. (1995) Single-crystal pulsed neutron diffraction of a highly hydrous beryl. *Acta Crystallographica*, **B51**, 733–737.

Aurisicchio, C., Fioravanti, G., Grubessi, O. and Zanazzi, P.F. (1988) Reappraisal of the crystal chemistry of beryl. *American Mineralogist*, **73**, 826–837.

Aurisicchio, C., Grubessi, O. and Zecchini, P. (1994) Infrared spectroscopy and crystal chemistry of the beryl group. *The Canadian Mineralogist*, **32**, 55–68.

Bragg, W.L. and West, J. (1926) The structure of beryl. *Proceedings of the Royal Society, London*, **3A**, 691–714.

Brown, G.E. Jr. and Mills, B.A. (1986) High-temperature structure and crystal chemistry of hydrous alkali-rich beryl from the Harding pegmatite, Taos County, New Mexico. *American Mineralogist*, **71**, 547–556.

Černý, P., Anderson, A.J., Tomascak, P.B. and Chapman, R. (2003) Geochemical and morphological features of beryl from the Bikita granitic pegmatite, Zimbabwe. *The Canadian Mineralogist*, **41**, 1003–1011.

Charoy, B., De Donato, P., Barres, O. and Pinto-Coelho, C. (1996) Channel occupancy in alkali-poor beryl from Serra Branca (Goias, Brasil): spectroscopic characterization. *American Mineralogist*, **81**, 395–403.

De Almeida Sampaio Filho, H., Sighinolfi, G. and Galli, E. (1973) Contribution to crystal chemistry of beryl. *Contributions to Mineralogy and Petrology*, **38**, 279–290.

Evdokimova, O.A., Belokoneva, E.L., Artemenko, V.V., Dubovskaya, V.M. and Urusov, V.S. (1989) Location of impurity cations in synthetic Co- and Cu-containing beryls according to results of precision X-ray structural analysis, ESR and optical spectroscopy. *Kristallografiya*, **34**, 723–730.

Farmer, V.C. (1974) *The Infrared Spectra of Minerals*. Mineralogical Society, London.

Ferraris, G., Prencipe, M. and Rossi, P. (1999) Stoppaniite, a new member of the beryl group: crystal structure and crystal-chemical implications. *European Journal of Mineralogy*, **10**, 491–496.

Fleet, M.E. (1981) The structure of magnetite. *Acta Crystallographica*, **B37**, 917–920.

Gatta, G.D., Nestola, F., Bromiley, G.D. and Mattauch, S. (2006) The real topological configuration of the extra-framework content in alkali-poor beryl: a multi-methodological study. *American Mineralogist*, **91**, 29–34.

Gibbs, G.V., Breck, D.W. and Meagher, E.P. (1968) Structural refinement of hydrous and anhydrous beryl, $Al_2(Be_3Si_6)O_{18}$ and emerald, $Al_{1.9}Cr_{0.1}(Be_3Si_6)O_{18}$. *Lithos*, **1**, 275–285.

Goldman, D.S., Rossman, G.R. and Parkin, K.M. (1978) Channel constituents in beryl. *Physics and Chemistry of Minerals*, **3**, 225–235.

Hawthorne, F.C. and Černý, P. (1977) The alkali-metal positions in Cs-Li beryl. *The Canadian Mineralogist*, **15**, 414–421.

Hazen, R.M., Au, A.Y. and Finger, L.W. (1986) High-pressure crystal chemistry of beryl ($Be_3Al_2Si_6O_{18}$) and euclase ($BeAlSiO_4OH$). *American Mineralogist*, **71**, 977–984.

Ismunandar, B.J.K. and Hunter, B.A. (1999) Phase transformation in $CuRh_2O_4$: a powder neutron diffraction study. *Materials Research Bulletin*, **34**, 135–143.

Koivula, J.I. and Kammerling, R.C. (1988) Gem News. Unusual synthetic beryls from the Soviet Union. *Gems and Gemology*, **24**, 252.

Koivula, J.I., Tannous, M. and Schmetzer, K. (2000) Synthetic gem materials and simulants in the 1990s. *Gems and Gemology*, **36**, 360–379.

Kolesov, B.A. and Geiger, C.A. (2000) The orientation and vibrational states of H_2O in synthetic alkali-free beryl. *Physics and Chemistry of Minerals*, **27**, 557–564.

Larson, A.C. (1970) *Crystallographic Computing* (F.R. Ahmed, S.R. Hall and C.P. Huber, editors). Munksgaard, Copenhagen, pp. 291–294.

Manier-Glavinaz, V., Couty, R. and Lagache, M. (1989) The removal of alkalis from beryl: structural adjustments. *The Canadian Mineralogist*, **27**, 663–671.

Mashkovtsev, R.I. and Smirnov, S.Z. (2004) The nature of channel constituents in hydrothermal synthetic emerald. *Journal of Gemmology*, **29**, 129–141.

Morosin, B. (1972) Structure and thermal expansion of beryl. *Acta Crystallographica*, **B28**, 1899–1903.

Nassau, K. (1990) Synthetic gem materials in the 1980s. *Gems and Gemology*, **26**, 50–63.

Oxford Diffraction (2005) *CrysAlis Software system, Version 1.170. Xcalibur CCD system*. Oxford Diffraction Ltd.

Prencipe, M. (2002) Ab initio Hartree-Fock study and charge density analysis of beryl ($Al_4Be_6Si_{12}O_{36}$). *Physics and Chemistry of Minerals*, **29**, 552–561.

Sanders, I.S. and Doff, D.H. (1991) A blue sodic beryl from southeast Ireland. *Mineralogical Magazine*, **55**, 167–172.

Schmetzer, K. (1989) Types of water in natural and synthetic emerald. *Neues Jahrbuch für Mineralogie Monatshefte*, **1**, 541–551.

Schmetzer, K. and Kiefert, L. (1990) Water in beryl – a contribution to the separability of natural from synthetic emeralds by infrared spectroscopy. *Journal of Gemmology*, **22**, 215–223.

Schmetzer, K., Schwarz, D., Bernhardt, H.-J. and Häger, T. (2006) A new type of Tairus hydrothermally-grown synthetic emerald, coloured by vanadium and copper. *Journal of Gemmology*, **30**, 59–74.

Sheldrick, G.M. (1997) *SHELX-97. Programs for crystal structure determination and refinement*. University of Göttingen, Germany.

Sheriff, B.L., Grundy, D.H., Hartman, J.S., Hawthorne, F.C. and Černý, P. (1991) The incorporation of alkalis in beryl: multi-nuclear MAS NMR and crystal structure study. *The Canadian Mineralogist*, **29**, 271–285.

Webster, R. (2006) *Gems: Their Sources, Descriptions and Identification*. 6th edition (M. O'Donoghue, editor). Butterworth-Heinemann, Oxford, UK.

Wilson, A.J.C. and Price, E. (Eds) (1999) *International Tables for Crystallography C*. Kluwer Academic Publishers, Dordrecht, The Netherlands.

Wood, D.L. and Nassau, K. (1967) Infrared spectra of foreign molecules in beryl. *Journal of Chemical Physics*, **42**, 2220–2228.

Wood, D.L. and Nassau, K. (1968) The characterization of beryl and emerald by visible and infrared absorption spectroscopy. *American Mineralogist*, **53**, 777–800.